miR-874 ameliorates retinopathy in diabetic rats by NF-κB signaling pathway

Rui Li
Xiaogan Hospital Affiliated to Wuhan University of Science and Technology
Huimin Yuan
Xiaogan Hospital Affiliated to Wuhan University of Science and Technology
Tao Zhao
Xiaogan Hospital Affiliated to Wuhan University of Science and Technology
Yimin Yan
Xiaogan Hospital Affiliated to Wuhan University of Science and Technology
Zhaochen Liu
Xiaogan Hospital Affiliated to Wuhan University of Science and Technology
Jiayu Cai
Xiaogan Hospital Affiliated to Wuhan University of Science and Technology
Chunli Qiu
Xiaogan Hospital Affiliated to Wuhan University of Science and Technology
Chuanjing Li (lichuanjing35gh@163.com)
Xiaogan Hospital Affiliated to Wuhan University of Science and Technology https://orcid.org/0000-0002-4773-3426

Research article

Keywords: diabetic retinopathy; Rela (p65); rat; miR-874; NF-κB

Posted Date: September 18th, 2019

DOI: https://doi.org/10.21203/rs.2.14609/v1

Version of Record: A version of this preprint was published at Advances in Clinical and Experimental Medicine on April 29th, 2021. See the published version at https://doi.org/10.17219/acem/130602.

Abstract

Background: This study aimed to explore the improvement effect of miR-874 on retinopathy in diabetic rats by NF-κB signaling pathway.

Methods: Ten healthy Sprague-Dawley rats were taken as the control group. Sixty streptozotocin (60 mg/kg)-induced diabetes model rats were randomly divided into model group (without any treatment), negative control (NC) agomir group (injection of overexpressed NC vector), miR-874 agomir group (injection of miR-874 mimic), miR-874 anti-agomir group (injection of miR-874 inhibitor), EVP4593 group (injection of NF-κB signaling pathway antagonist EVP4593), and miR-874 anti-agomir + EVP4593 group (injection of miR-874 inhibitor and EVP4593). All injection was via caudal vein.

Results: miR-874 could target the degradation of p65. Compared with control group, there were significantly reduced miR-874 expression, increased VEGF and Ang2 protein expressions, lowered end-diastolic velocity and peak systolic velocity of central retinal artery (CRA), and blood velocity of central retinal vein and CRA, heightened plasma viscosity, blood viscosity and erythrocyte sedimentation rate at all shear rates, decreased capillary pericytes, increased vascular endothelial cells, and ascended p65 expression in the retina of rats in model group (all $P < 0.05$). It showed that pathological changes were happened on the retina of diabetes rats. These indexes showed the same results after miR-874 was inhibited (all $P < 0.05$). However, these indexes showed the opposite results in miR-874 agomir group and EVP4593 group compared with model group (all $P < 0.05$). EVP4593 could alleviate the aggravation of retinopathy caused by the inhibition of miR-874 in diabetes rats.

Conclusions: miR-874 mediates NF-κB signaling pathway by targeting the degradation of p65 to further improve the retina of diabetes rats, showing the improvement effect of miR-874 on diabetic retinopathy in rats.

Background

China is a country with a high incidence of diabetes, and there are over 100 million patients with diabetes. Diabetes can induce retinopathy, which is an important reason why diabetes can cause visual disturbance and even blindness [1–3]. Diabetic retinopathy (DR) is a kind of microvascular complication, and it is triggered by the leakage of retinal capillary wall that is caused by the hyperglycemia of diabetic patients. However, its pathogenesis is complicated and not fully understood. Previous studies suggested that a series of pathophysiological changes had happened on the retina under the stimulation of persistent hyperglycemia, resulting in retinopathy [4–8].

Several studies have showed that the activity of NF-κB signaling pathway is significantly increased in diabetes rats, and the up-regulation of NF-κB p65 expression augments the generation of reactive oxygen species and further leads to the occurrence of microaneurysms, retinal neovascularization and vitreous hemorrhage, boosting the progression of retinopathy in diabetes rats [9–11]. Encoded by endogenous gene, microRNA (miRNA) is a non-coding single-stranded RNA molecule (containing about 21–23

nucleotides) and has the features of high conservation, time sequence and tissue specificity [12, 13]. miRNAs can interact with the 3'UTR region of the specific target gene by sequence-specific mode to regulate the protein expression of target gene. Recent studies have revealed that miRNA participates in the development and progression of DR and is involved in multiple pathogenesis of DR [14–16]. We found that there was the binding site between miR–874 and NF-κB p65 by the prediction on a bioinformatics website, and that the down-regulation of miR–874 expression in myocardial ischemia reperfusion injury of rats exerted an inhibitory effect on inflammation and injury [17, 18]. However, we did not found the relationship between miR–874 and DR. Therefore, it was unknown whether miR–874 regulated DR and whether NF-κB p65 acted as a downstream regulatory element for miR–874 in DR.

In this study, DR rat models were established and treated to explore the effect of miR–874 on DR rats and the regulatory relationship between miR–874 and NF-κB signaling pathway. The results were conducive to further understand the pathogenesis of DR and provided a theoretical foundation for miR–874 to become a potential target for new drugs in the treatment of DR.

Methods

Cell culture

HEK293T cells from the American Type Culture Collection were used for dual-luciferase reporter assay. HEK293T cells were cultured in DMEM containing 10% fetal bovine serum by routine method. Cells were passaged and cultured in fresh complete medium every three days.

Dual-luciferase reporter assay

The binding site of miR–874 and Rela (p65) was analyzed on a bioinformatics prediction website (www.targetscan.org). Then the target relationship between miR–874 and Rela was verified by dual-luciferase reporter system. The gene vector of target gene Rela in dual-luciferase reporter system and the mutant in the binding site of miR–874 and Rela were constructed: pmirGLO-Rela wt and pmirGLO-Rela mut. These two reporter plasmid and NC mimic or miR–874 mimic were co-transfected into HEK 293T cells respectively. After 24 h cell transfection, dual-luciferase reporter assay was performed. Cells were lysed and centrifuged at 12,000 rpm for 1 min. The sediment was discarded, and the supernatant was collected. Luciferase activity was measured according to the instruction of dual-luciferase reporter assay kit (Promega). Operating steps were as follows. Lysed cells were pipetted into Eppendorf tubes. Every 10 μl cells were added with 100 μl firefly luciferase working solutions to measure firefly luciferase activity followed by the addition of 100 μl renilla luciferase working solutions to detect renilla luciferase activity. Relative luciferase activity = firefly luciferase activity / renilla luciferase activity.

Establishment of diabetes rat models

Streptozotocin (STZ) was used to induce diabetes rat models. Ninety male Sprague-Dawley rats (200–250 g, 8 weeks old, from the Laboratory Animal Center of Chongqing Medical University, China) were fed with standard food and water in the laboratory under specific pathogen free condition. Ten rats were randomly selected as control group, and the rest were used to construct models. Citrate buffer solutions (pH 4.5) were used to prepare fresh STZ solutions. Single intraperitoneal injection of 60 mg/kg STZ solutions was performed in rats to induce diabetes. One week later, rats with fasting blood glucose above 250 mg/dl were considered to be successfully modeled [19]. There were 71 successfully modeled rats. The protocol and procedures employed were performed, ethically reviewed and approved by the Ethics Committee of Xiaogan Central Hospital (2017010) and in compliance with the statement of Association for Research in Vision and Ophthalmology for the care and use of laboratory animals in ophthalmology and vision studies. All rats were anesthetized to collect the eyeballs after modeling followed by euthanasia.

Grouping and disposing

Sixty successfully modeled rats were randomly selected and divided into 6 groups with 10 rats in each group. There were 7 groups in this study: control group (healthy rats), model group (model rats, without any treatment), negative control (NC) agomir group (model rats, injection of overexpressed NC vector via caudal vein), miR–874 agomir group (model rats, injection of miR–874 mimic via caudal vein), miR–874 anti-agomir group (model rats, injection of miR–874 inhibitor via caudal vein), EVP4593 group (model rats, injection of NF-κB signaling pathway antagonist EVP4593 via caudal vein), and miR–874 anti-agomir + EVP4593 group (model rats, injection of miR–874 inhibitor and EVP4593). The above mimics and antagonists of 80 mg/kg at a concentration of 4.5 nM were injected into rats via caudal vein, once every three days for 4 weeks [20]. Eight weeks later, rats were fasted for 8 h. Then blood was drawn via caudal vein, and blood glucose was measured using One Touch II glucometer (USA). Rats were weighed. The experiment was performed in triplicate.

Retinal hemodynamic indexes and central artery hemorheology indexes detection in diabetes rats

Nine weeks after grouping, the rat eyeball was detected by color Doppler ultrasound, and hemodynamic indexes of the left eye such as end-diastolic velocity (EDV), peak systolic velocity (PSV) and central retinal vein (CRV) were detected in all rats. Anticoagulated blood was drawn via abdominal aorta after rats were fasted for 20 h. Plasma viscosity (PV), blood viscosity (BV) and erythrocyte sedimentation rate (ESR) at different shear rates were measured using blood viscometer.

Detection of number of retinal vascular endothelial cells and pericytes

The eyeballs of all rats were extirpated and fixed. Retinal vascular digest preparations were performed. Number of retinal vascular endothelial cells (VEC) and capillary pericytes (IPC) was counted using a microscope.

Separation of retinal tissue

General anesthesia was performed on rats by intraperitoneal injection of 1% pentobarbital sodium before the separation of retina. Surface anesthesia was performed on the eye using oxybuprocaine hydrochloride eye drops. Then the eyeballs of rats were extirpated under aseptic conditions. The bulbar conjunction was removed. The cornea was separated 1 mm from the posterior of corneoscleral limbus followed by the evisceration of crystalline lens and the removal of vitreous body under a stereomicroscope. The retina was isolated along the underpart of the retina, and the optic nerve was cut off. The retina was dissociated and cut into pieces.

qRT-PCR

Total RNA in the retina was extracted by Trizol method (Invitrogen, Calsbad, CA, USA). The ratios of A_{260}/A_{230} and A_{260}/A_{280} were measured by nanodrop2000 micro-ultraviolet spectrophotometer (1011U, nanodrop, USA) to determine the concentration and purity of total RNA. RNA was reversely transcribed into cDNA according to the instruction of TaqMan MicroRNA Assays Reverse Transcription primer (4427975, Applied Biosystems, USA). cDNA was diluted to 50 ng/μl, for 2 μl every time, and amplification reaction solutions were 25 μl. Reverse transcription reaction conditions: reacting at 37 °C for 30 min and at 85 °C for 5 s. Primers of CCL22 were synthesized by Wuhan Branch of Sangon Biotech (Shanghai) Co., Ltd., China (Table 1). Real-time fluorescence quantitative polymerase chain reaction (qRT-PCR) was performed using an ABI7500 quantitative PCR amplifier (7500, ABI, USA). Reaction conditions: pre-denaturation at 95 °C for 10 min followed by 40 circles of denaturation at 95 °C for 10 s, annealing at 60 °C for 20 s and extending at 72 °C for 34 s. Fluorescence quantitative PCR amplification solutions were 20 μl, including 10 μl SYBR Premix Ex Taq^{TM} II, 0.8 μl PCR forward primer (10 μM), 0.8 μl PCR reverse primer (10 μM), 0.4 μl ROX Reference Dye II, 2.0 μl cDNA templates, and 6.0 μl sterilized distilled water. U6 was used as the internal reference to analyze the relative expression of miR−195, and GAPDH was used as the internal reference to analyze the relative expressions of CD40, RORyt, Foxp3, interleukin (IL) −17, IL−10, tumor necrosis factor (TNF)-α, IL−23 and IL−8. $2^{-\Delta\Delta Ct}$ showed the relative expression of target gene. $\Delta\Delta Ct = \Delta Ct_{experimental\ group} - \Delta Ct_{GAPDH}$. $\Delta Ct = Ct_{target\ gene} - Ct_{internal\ reference}$. Ct represented amplification circles as the real-time fluorescence intensity of the reaction reached the threshold value. The experiment was performed in triplicate.

Western blotting

p65 expression was detected by Western blotting. RIPA (Beyotime Biotechnology Co., Ltd., China) was mixed with protease inhibitor and PMSF to lyse cells on the ice for 30 min. Cells were scraped into 1.5 ml Eppendorf tubes with a cell scraper and centrifuged at 10,000 rpm and 4 °C for 15 min. Protein concentration was measured using BCA protein assay kit (Beijing Dingguo Changsheng Biotechnology Co., Ltd., China). Protein was separated by SDS-PAGE for 2 h and transferred to PVDF membranes. The membrane was sealed with 5% milk for 2 h and incubated at 4 °C with the addition of primary antibodies including rabbit anti-human polyclonal antibodies angiopoietin2 (Ang2) (1:2,500, ab155106, Abcam, USA), p65 (1:2,500, ab32536, Abcam, USA), vascular endothelial growth factor (VEGF) (1:2,500, ab1316, Abcam, USA) and GAPDH (1:2,500, ab9485, Abcam, USA). After cells were washed with tris buffered saline tween (TBST) three times, horse radish peroxidase-labeled IgG (1:10,000, ab6721, Abcam, USA) was added and incubated at room temperature for 1 h. Then cells were washed with TBST three times. Color development was carried out by electrogenerated chemiluminescence solution. Relative expression of protein = gray value of target protein band / gray value of GAPDH band.

Statistical analysis

SPSS 11.5 software was used to analyze the data. The measurement data were expressed as mean ± standard deviation. Comparison among groups was performed by one-way ANOVA in conjunction with post-hoc LSD-t test. $P < 0.05$ was considered to be statistically significant.

Results

Dual-luciferase reporter assay results

There was the binding site between miR−874 and Rela (p65) by predicting on a bioinformatics website (Fig. 1A). Dual-luciferase reporter assay results showed that there was no significant difference in 3′-UTR co-transfection between miR−874 and mutational p65, and 3′-UTR co-transfection of miR−874 and wild-type p65 significantly reduced luciferase activity (Fig. 1B), indicating the target regulation of miR−874 on p65.

Symptoms and retinal injury relief of STZ-induced diabetes rats using miR−847

Seventy-one rats were successfully modeled, fed and closely monitored. Rats' blood glucose levels were measured after modeling. Blood glucose level was increased in model group and normal in control group at about 4 mmol/l; the soaring of modeled rats' blood glucose was slowed down in miR−874 agomir group and EVP4593 group; the soaring of modeled rats' blood glucose was facilitated in miR−874 anti-agomir group; EVP4593 neutralized the promotion of miR−847 anti-agomir on modeled rats' blood glucose in miR−874 anti-agomir + EVP4593 group (Fig. 2A).

Compared with control group, rat weight in model group was not significantly increased with time. Rat weight in control group was in regular growth. The increase of rat weight was accelerated in miR–874 agomir group and EVP4593 group; the increase of rat weight was inhibited in miR–874 anti-agomir group; EVP4593 neutralized the inhibition of miR–847 anti-agomir on rat weight in miR–874 anti-agomir + EVP4593 group (Fig. 2B).

Ang2 and VEGF could reflect the degree of retinal injury to some extent. VEGF as an angiogenesis factor is related to the angiogenesis of retina; Ang2 could promote the retinal vascular permeability. The abnormal expression of Ang2 and VEGF could cause retinal vascular endothelial cell damage and pro-inflammatory response. The expressions of VEGF and Ang2 were detected by Western Blotting (Fig. 2C and D). VEGF and Ang2 expressions were significantly increased in the retina of model group ($P < 0.05$), indicating that pathological changes were happened on the retina. VEGF and Ang2 protein expressions were inhibited in miR–874 agomir group and EVP4593 group; VEGF and Ang2 protein expressions were promoted in miR–874 anti-agomir group; EVP4593 neutralized the promotion of miR–847 anti-agomir on VEGF and Ang2 protein expressions in miR–874 anti-agomir + EVP4593 group.

Retinopathy relief of diabetes rats using miR–847

Hemodynamic indexes of rats with DR were measured to detect retinal blood perfusion and blood supply. Compared with control group, CRV, EDV and PSV values in model group were decreased in varying degrees, indicating that insufficient retinal blood perfusion and blood supply was occurred in model group. Compared with NC agomir group, CRV, EDV and PSV values were higher in miR–874 agomir group and EVP4593 group, and CRV, EDV and PSV values were lower in miR–874 anti-agomir group; EVP4593 neutralized the inhibition of miR–847 anti-agomir on CRV, EDV and PSV values in miR–874 anti-agomir + EVP4593 group (all $P < 0.05$). It manifested that miR–874 had an influence on hemodynamic indexes of rats with DR, and miR–874 could alleviate retinopathy of diabetes rats (Fig. 3).

Hemorheology indexes of rats with DR were measured to further verify the alleviation of miR–874 on DR (Fig. 4). Compared with control group, ESR, BV and PV were increased in model group. Compared with NC agomir group, ESR, BV and PV were significantly reduced in miR–874 agomir group and EVP4593 group; ESR, BV and PV at all shear rates were accelerated in miR–874 anti-agomir group; EVP4593 neutralized the promotion of miR–847 anti-agomir on BV, PV and ESR at all shear rates in miR–874 anti-agomir + EVP4593 group (all $P < 0.05$). It demonstrated that miR–874 relieved retinopathy of diabetes rats.

Number of retinal capillary VEC and IPC was detected. Compared with control group, number of IPC was significantly reduced, and number of VEC was significantly increased in the retinal capillary in model group. Compared with NC agomir group, number of IPC was raised, and VEC proliferation was decreased in the retinal capillary in miR–874 agomir group and EVP4593 group, with a significant difference (Fig. 5). Number of IPC was significantly reduced, and VEC proliferation was significant in the retinal capillary in mir–847 anti-agomir group; EVP4593 neutralized the IPC number decrease and VEC proliferation that

caused by miR–847 anti-agomir in miR–874 anti-agomir + EVP4593 group (all $P < 0.05$). It showed that miR–874 relieved retinopathy of diabetes rats.

p65 expression in the retina of diabetes rats affected by miR–874

Total RNA and total protein in the retina were extracted. miR–874 expression was detected by qRT-PCR. Rela (p65) protein expression was measured by Western blot. The results were shown in Fig. 6. Compared with control group, miR–874 expression was significantly decreased, and p65 expression was significantly increased in the retina in model group. Compared with NC agomir group, miR–874 expression was significantly elevated in miR–874 agomir group, and there was no significant difference in miR–874 expression in EVP4593 group. p65 expression was significantly inhibited in miR–874 agomir group and EVP4593 group. p65 expression was significantly increased after the inhibition of miR–874. EVP4593 balanced the promotion of miR–874 anti-agomir on p65 in miR–874 anti-agomir + EVP4593 group. It suggested that miR–874 inhibited NF-κB signaling pathway by suppressing p65, exerting improvement effect on DR in rats.

Discussion

Diabetes is a prevalent disease occurred in most of the world's population. Neuropathy, microangiopathy and macroangiopathy are main pathological features of diabetes complications. DR is the most common diabetes complication. It is caused by retinal vascular leakage, inflammatory response and neovascularization. DR is also the leading cause of blindness in working-age population around the world. The main methods for the treatment of DR are laser photocoagulation treatment, hyperbaric oxygen therapy and drug therapy [21]. However, these methods may lead to adverse side effects such as visual acuity decrease, contrast sensitivity decrease and visual field damage. Therefore, the more efficient therapeutic strategies are needed to be developed for DR patients.

NF-κB is a nuclear transcription factor and participates in the generation process of multiple cytokines [22, 23]. It mainly plays a role in biological processes such as biological immunity and inflammation. NF-κB includes five members: RelB, RelA (also known as p65), c-Rel, p100/p52 and p105/p50. p65–50 is the most widespread and most important NF-κB heterodimer [24–26]. The retina experiences many metabolic disorders, and changes have happened on gene expressions. The progression of diabetes can result in retinal capillary cell death and histopathological changes. Many studies found that NF-κB was activated in the retina of diabetes, and the activated NF-κB increased capillary cell apoptosis [27], which was anterior to the development of histopathological features of DR [28]. Once NF-κB was activated in the pathogenesis of early DR, its function could only be inhibited partially by early reconstruction. Moreover, if the hyperglycemia induced by diabetes was not well controlled for 7 months, it could be irreversible. In this study, there were heightened EDV, PSV of central retinal artery (CRA), and blood velocity of CRV, lowered PV, BV and ESR at all shear rates, increased number of retinal capillary pericytes,

decreased endothelial cell proliferation, and significantly reduced p65 expression in the retina in EVP4593 group as compared to model group. It indicated that the inhibition of NF-κB signaling pathway significantly improved the condition of DR in rats, which was consistent with the results in the literature we reviewed.

Recently, microRNA has been identified as a biomarker for the diagnosis of various diseases including DR. Moreover, there is growing evidence that miRNA plays a key role in regulating NF-κB activation and downstream function. However, the mechanism of miRNA on NF-κB activation or inhibition in DR has not been fully revealed. Many recent studies have showed that miR–874 plays a role in various diseases, and miR–874 is involved in several types of cancers, such as colorectal cancer, gastric cancer and non-small cell lung cancer [29]. miR–874 is significantly down-regulated in sertoli cells of diabetes rats and rats induced by glucose, and miR–874 overexpression relieves the renal injury of diabetes rats [30]. However, there is no study on the relationship between miR–874 and DR. In this study, bioinformatics predicted that there was the targeted binding site between miR–874 and p65 which was the most important protein in NF-κB signaling pathway. Moreover, experiments confirmed that p65 was a target gene of miR–874. Furthermore, DR model in Sprague-Dawley rats was successfully established to explore the relationship between miR–874 and NF-κB signaling pathway in DR rats. The results showed that DR rats after the treatment of overexpressed miR–874 mimic had increased EDV, PSV of CRA and blood velocity of CRV, lowered PV, BV and ESR at all shear rates, increased number of retinal capillary pericytes, decreased endothelial cell proliferation, and significantly reduced p65 expression in the retina. DR was aggravated after the treatment of miR–874 inhibitor for diabetes rats. NF-κB signaling pathway antagonist EVP4593 counteracted the aggravation of retinopathy caused by miR–874 inhibitor. The results indicated that miR–874 overexpression inhibited the expression of NF-κB signaling pathway, alleviating retinopathy in diabetes rats.

Conclusions

miR–874 can inhibit p65, an important protein in NF-κB signaling pathway, in the retina of diabetes rats and further inhibit NF-κB signal, playing an alleviation effect on retinopathy. miR–874 may be a new targeted drug for the improvement of DR. In this study, the effect of miR–874 on retinopathy in diabetes rats has been confirmed, while the specific molecular mechanism between miR–874 and NF-κB is not clear. Moreover, whether overexpressed miR–874 mimic can be applied in clinical treatment still needs more experimental verification.

Abbreviations

DR: diabetic retinopathy; miRNA: microRNA; STZ: Streptozotocin; NC: negative control; EDV: end-diastolic velocity; PSV: peak systolic velocity; CRV: central retinal vein; PV: plasma viscosity; BV: blood viscosity; ESR: erythrocyte sedimentation rate; VEC: vascular endothelial cells; IPC: capillary pericytes; qRT-PCR: real-time fluorescence quantitative polymerase chain reaction; IL: interleukin; TNF: tumor necrosis factor;

Ang2: angiopoietin2; VEGF: vascular endothelial growth factor; TBST: tris buffered saline tween; CRA: central retinal artery

Declarations

Acknowledgments

Not applicable.

Funding

Not applicable.

Availability of data and materials

The datasets used and/or analyzed during the current study are available from the corresponding author on reasonable request.

Author’s contributions

RL contributed to conception and design and drafted the article. HMY and TZ designed the study and revised the article for important intellectual content. YMY and ZCL analyzed and interpreted of data and drafted the article. JYC and CLQ acquired the data and drafted the article. CJL contributed to conception and design and revised the article for important intellectual content. All authors have read and approved the manuscript.

Ethical approval and consent to participate

The protocol and procedures employed were performed, ethically reviewed and approved by the Ethics Committee of Xiaogan Central Hospital (2017010) and in compliance with the statement of Association for Research in Vision and Ophthalmology for the care and use of laboratory animals in ophthalmology and vision studies.

Consent for publication

Not applicable.

Competing interests

The authors declare that they have no competing interests.

References

1.Brinchmann-Hansen O, Dahl-Jorgensen K, Hanssen KF, Sandvik L. The response of diabetic retinopathy to 41 months of multiple insulin injections, insulin pumps, and conventional insulin therapy. Archives of ophthalmology (Chicago, Ill: 1960). 1988;106(9):1242–6.

2.Xie MY, Yang Y, Liu P, Luo Y, Tang SB. 5-aza–2'-deoxycytidine in the regulation of antioxidant enzymes in retinal endothelial cells and rat diabetic retina. International journal of ophthalmology. 2019;12(1):1–7.

3.Obeid A, Su D, Patel SN, Uhr JH, Borkar D, Gao X, et al. Outcomes of Eyes Lost to Follow-up with Proliferative Diabetic Retinopathy That Received Panretinal Photocoagulation versus Intravitreal Anti-Vascular Endothelial Growth Factor. Ophthalmology. 2019;126(3):407–13.

4.Joussen AM, Poulaki V, Mitsiades N, Kirchhof B, Koizumi K, Dohmen S, et al. Nonsteroidal anti-inflammatory drugs prevent early diabetic retinopathy via TNF-alpha suppression. FASEB journal: official publication of the Federation of American Societies for Experimental Biology. 2002;16(3):438–40.

5.Zheng L, Szabo C, Kern TS. Poly(ADP-ribose) polymerase is involved in the development of diabetic retinopathy via regulation of nuclear factor-kappaB. Diabetes. 2004;53(11):2960–7.

6.Kamble VV KR. Automatic Identification and Classification of Microaneurysms, Exudates and Blood Vessel for Early Diabetic Retinopathy Recognition: Computational Intelligence in Data Mining. 2019.

7.Hemanth DJ DO, Kose U. An enhanced diabetic retinopathy detection and classification approach using deep convolutional neural network. Neural Computing and Applications. 2019(7398):1–15.

8.Thomas AA, Biswas S, Feng B, Chen S, Gonder J, Chakrabarti S. lncRNA H19 prevents endothelial-mesenchymal transition in diabetic retinopathy. Diabetologia. 2019;62(3):517–30.

9.Luo DW, Zheng Z, Wang H, Fan Y, Chen F, Sun Y, et al. UPP mediated Diabetic Retinopathy via ROS/PARP and NF-kappaB inflammatory factor pathways. Current molecular medicine. 2015;15(8):790–9.

10.Chen F, Zhang HQ, Zhu J, Liu KY, Cheng H, Li GL, et al. Puerarin enhances superoxide dismutase activity and inhibits RAGE and VEGF expression in retinas of STZ-induced early diabetic rats. Asian Pacific journal of tropical medicine. 2012;5(11):891–6.

11.Yin Y, Chen F, Wang W, Wang H, Zhang X. Resolvin D1 inhibits inflammatory response in STZ-induced diabetic retinopathy rats: Possible involvement of NLRP3 inflammasome and NF-kappaB signaling pathway. Molecular vision. 2017;23:242–50.

12.Liang Z, Gao KP, Wang YX, Liu ZC, Tian L, Yang XZ, et al. RNA sequencing identified specific circulating miRNA biomarkers for early detection of diabetes retinopathy. American journal of physiology Endocrinology and metabolism. 2018;315(3):E374-e85.

13.Zhang J, Wu L, Chen J, Lin S, Cai D, Chen C, et al. Downregulation of MicroRNA 29a/b exacerbated diabetic retinopathy by impairing the function of Muller cells via Forkhead box protein O4. Diabetes & vascular disease research. 2018;15(3):214–22.

14.Wang W, Lo ACY. Diabetic Retinopathy: Pathophysiology and Treatments. International journal of molecular sciences. 2018;19(6).

15.Sorrentino FS, Matteini S, Bonifazzi C, Sebastiani A, Parmeggiani F. Diabetic retinopathy and endothelin system: microangiopathy versus endothelial dysfunction. Eye (London, England). 2018;32(7):1157–63.

16.Meerson A, Eliraz Y, Yehuda H, Knight B, Crundwell M, Ferguson D, et al. Obesity impacts the regulation of miR–10b and its targets in primary breast tumors. BMC cancer. 2019;19(1):86.

17.Chen PJ, Shang AQ, Yang JP, Wang WW. microRNA–874 inhibition targeting STAT3 protects the heart from ischemia-reperfusion injury by attenuating cardiomyocyte apoptosis in a mouse model. Journal of cellular physiology. 2019;234(5):6182–93.

18.Yao T, Zha D, Gao P, Shui H, Wu X. MiR–874 alleviates renal injury and inflammatory response in diabetic nephropathy through targeting toll-like receptor–4. Journal of cellular physiology. 2018;234(1):871–9.

19.Gong Q, Li F, Xie J, Su G. Upregulated VEGF and Robo4 correlate with the reduction of miR–15a in the development of diabetic retinopathy. Endocrine. 2019.

20.Wang G, Yan Y, Xu N, Hui Y, Yin D. Upregulation of microRNA–424 relieved diabetic nephropathy by targeting Rictor through mTOR Complex2/Protein Kinase B signaling. Journal of cellular physiology. 2019;234(7):11646–53.

21.Berteau F, Rouviere B, Nau A, Le Berre R, Sarrabay G, Touitou I, et al. 'A20 haploinsufficiency (HA20): clinical phenotypes and disease course of patients with a newly recognised NF-kB-mediated autoinflammatory disease'. Annals of the rheumatic diseases. 2019;78(5):e35.

22.Aeschlimann FA, Laxer RM. Response to: 'A20 haploinsufficiency (HA20): clinical phenotypes and disease course of patients with a newly recognised NF-kB-mediated autoinflammatory disease' by Aeschlimann et al. Annals of the rheumatic diseases. 2019;78(5):e36.

23.Huang WJ, Wang Y, Liu S, Yang J, Guo SX, Wang L, et al. Retraction notice to "Silencing circular RNA hsa_circ_0000977 suppresses pancreatic ductal adenocarcinoma progression by stimulating miR–874–3p and inhibiting PLK1 expression" [Cancer Letters 422C (2018) 70–80]. Cancer letters. 2018;438:232.

24.Tang W, Wang W, Zhao Y, Zhao Z. MicroRNA–874 inhibits cell proliferation and invasion by targeting cyclin-dependent kinase 9 in osteosarcoma. Oncology letters. 2018;15(5):7649–54.

25.Liao H, Pan Y, Pan Y, Shen J, Qi Q, Zhong L, et al. MicroRNA874 is downregulated in cervical cancer and inhibits cancer progression by directly targeting ETS1. Oncology reports. 2018;40(4):2389–98.

26.Zhang Y, Wang X, Zhao Y. MicroRNA874 prohibits the proliferation and invasion of retinoblastoma cells by directly targeting metadherin. Molecular medicine reports. 2018;18(3):3099–105.

27.Antzelevitch C. Genetic, molecular and cellular mechanisms underlying the J wave syndromes. Cardiac Electrophysiology: from Cell to Bedside. 2018;76(5):483–93.

28.Jiang T, Guan LY, Ye YS, Liu HY, Li R. MiR–874 inhibits metastasis and epithelial-mesenchymal transition in hepatocellular carcinoma by targeting SOX12. American journal of cancer research. 2017;7(6):1310–21.

29.Yang R, Li P, Zhang G, Lu C, Wang H, Zhao G. Long Non-Coding RNA XLOC_008466 Functions as an Oncogene in Human Non-Small Cell Lung Cancer by Targeting miR–874. Cellular physiology and biochemistry: international journal of experimental cellular physiology, biochemistry, and pharmacology. 2017;42(1):126–36.

30.Leong KW, Cheng CW, Wong CM, Ng IO, Kwong YL, Tse E. miR–874–3p is down-regulated in hepatocellular carcinoma and negatively regulates PIN1 expression. Oncotarget. 2017;8(7):11343–55.

Table 1

Table 1 Primer sequence

Gene	Primer sequence (5’-3’)
miR-874	Forward: GGGCGGCCCCACGCACCA
	Reverse: GTGCAGGGTCCGAGGT
U6	Forward: CTCGCTTCGGCAGCACA
	Reverse: AACGCTTCACGAATTTGCGT

Figures

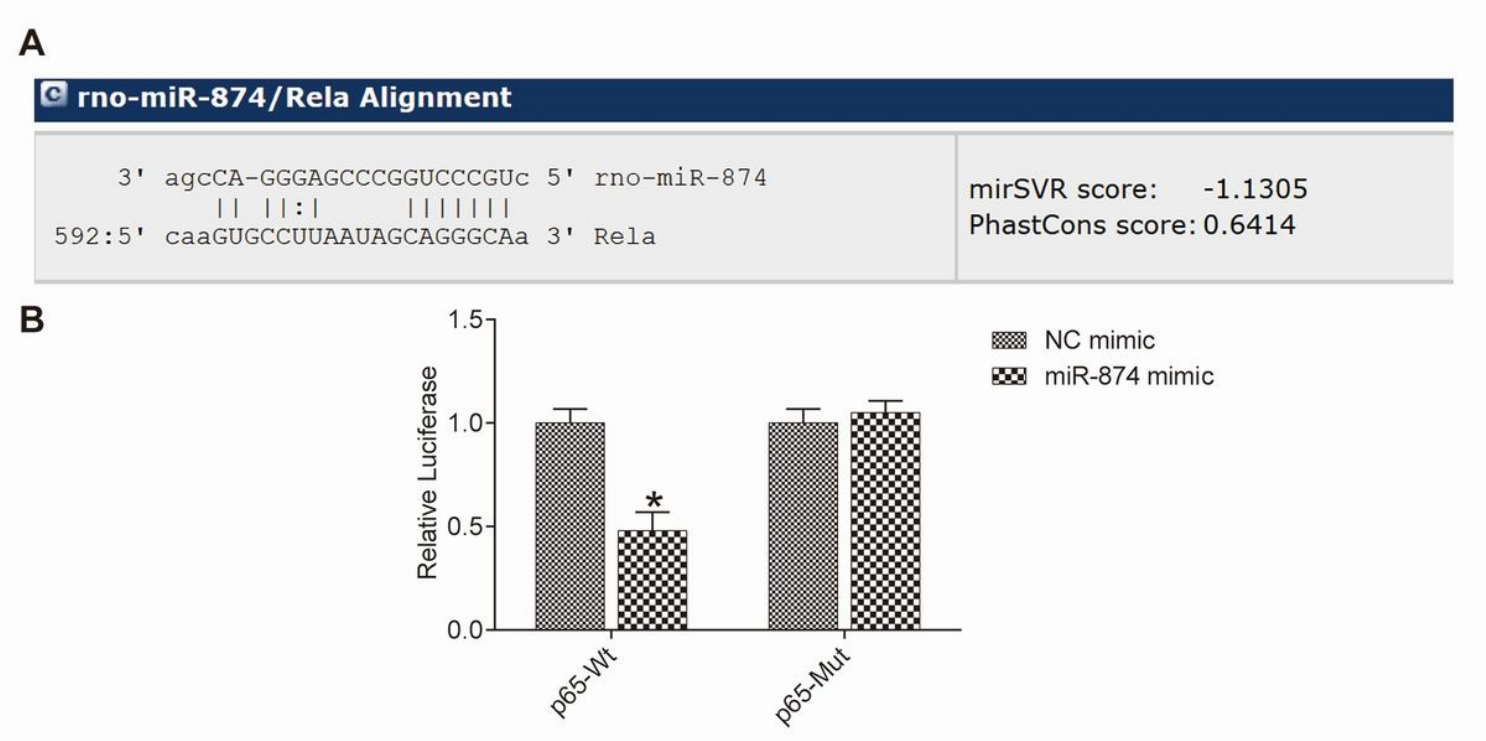

Figure 1

Bioinformatics prediction and dual-luciferase reporter assay results. A: There was the binding site between miR-874 and p65 by predicting on a bioinformatics website; B: There was a target relationship between miR-874 and p65 by the verification of dual-luciferase reporter assay. Compared with NC mimic group, *P < 0.05. NC negative control; Wt wild type; Mut mutant

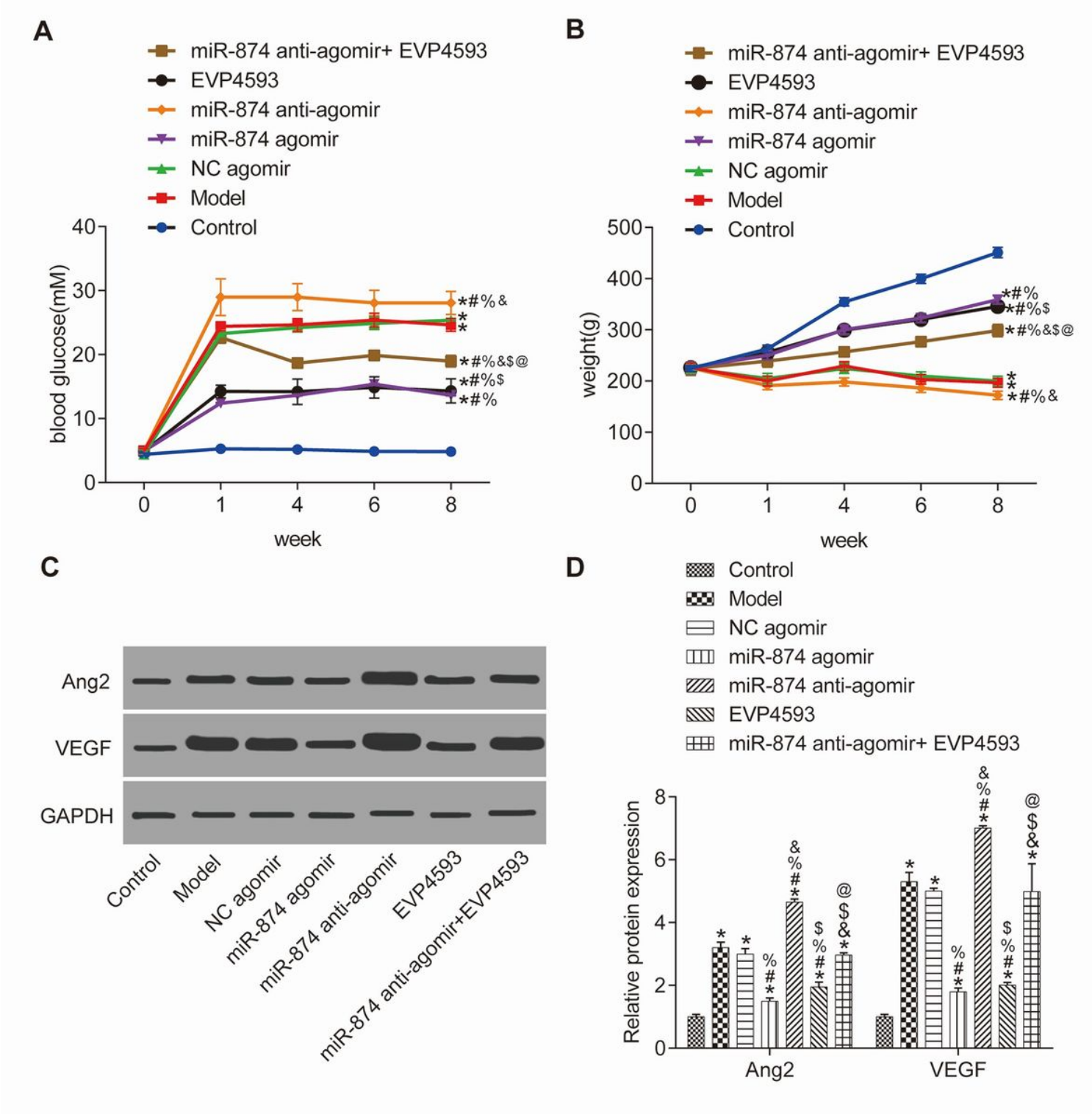

Figure 2

Retinal pathological changes detection. A: Blood glucose; B: Weight; C: Protein bands of Ang2 and VEGF in the retina of STZ-induced diabetes rat models; D: Protein expression histogram. Compared with control group, *P < 0.05; compared with model group, #P < 0.05; compared with NC agomir group, %P < 0.05; compared with miR-874 agomir group, &P < 0.05; compared with miR-874 anti-agomir group, $P < 0.05;

compared with EVP4593 group, @P < 0.05. NC negative control; VEGF vascular endothelial growth factor; Ang2 angiopoietin2; STZ streptozotocin

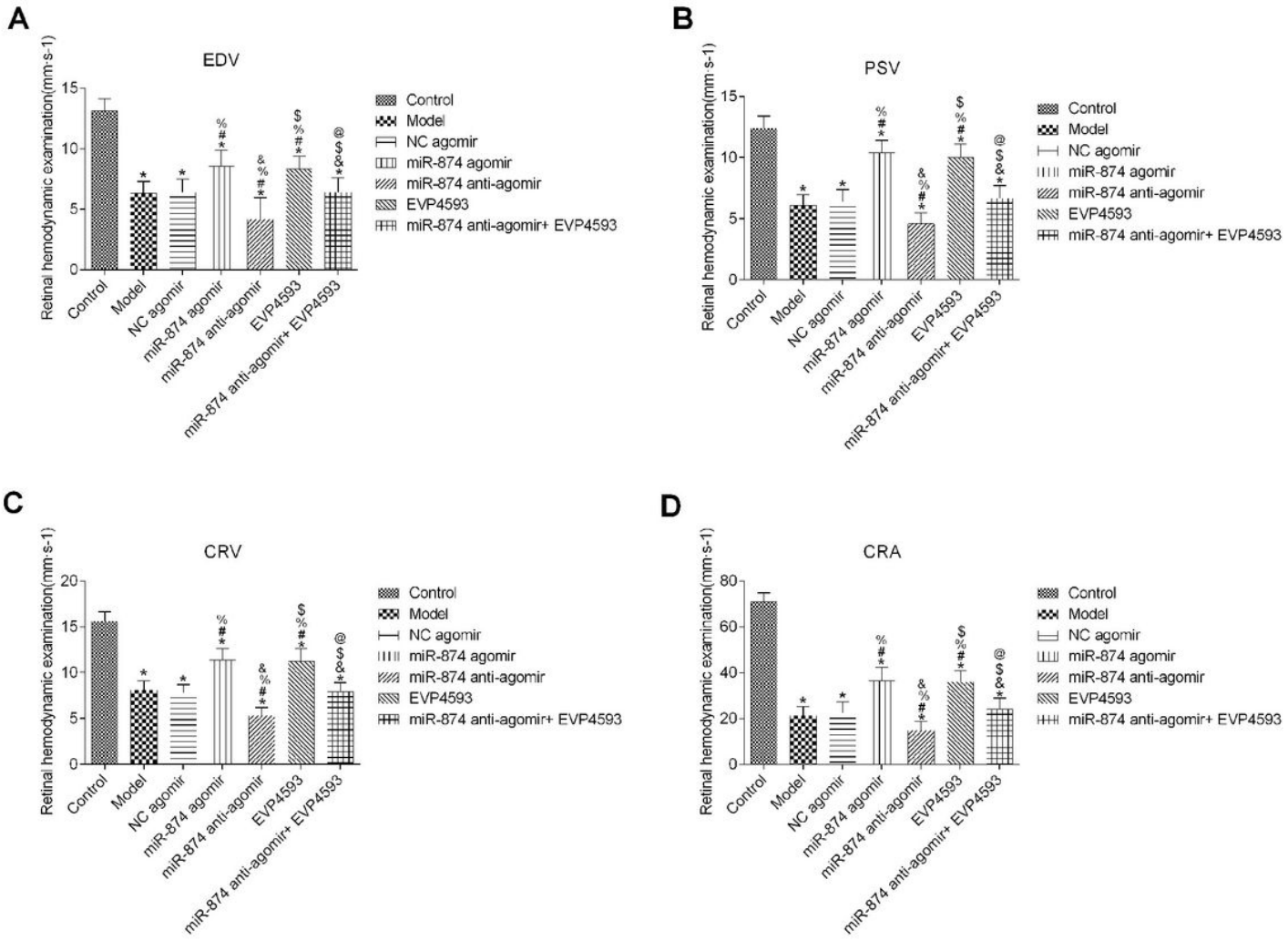

Figure 3

Retinal hemodynamic examinations of diabetes rats. A: End-diastolic velocity; B: Peak systolic velocity of central retinal artery; C: Blood velocity of central retinal vein; D: Blood velocity of central retinal artery. Compared with control group, *P < 0.05; compared with model group, #P < 0.05; compared with NC agomir group, %P < 0.05; compared with miR-874 agomir group, &P < 0.05; compared with miR-874 anti-agomir group, $P < 0.05; compared with EVP4593 group, @P < 0.05. NC negative control; EDV end-diastolic velocity; PSV peak systolic velocity; CRV central retinal vein; CRA central retinal artery

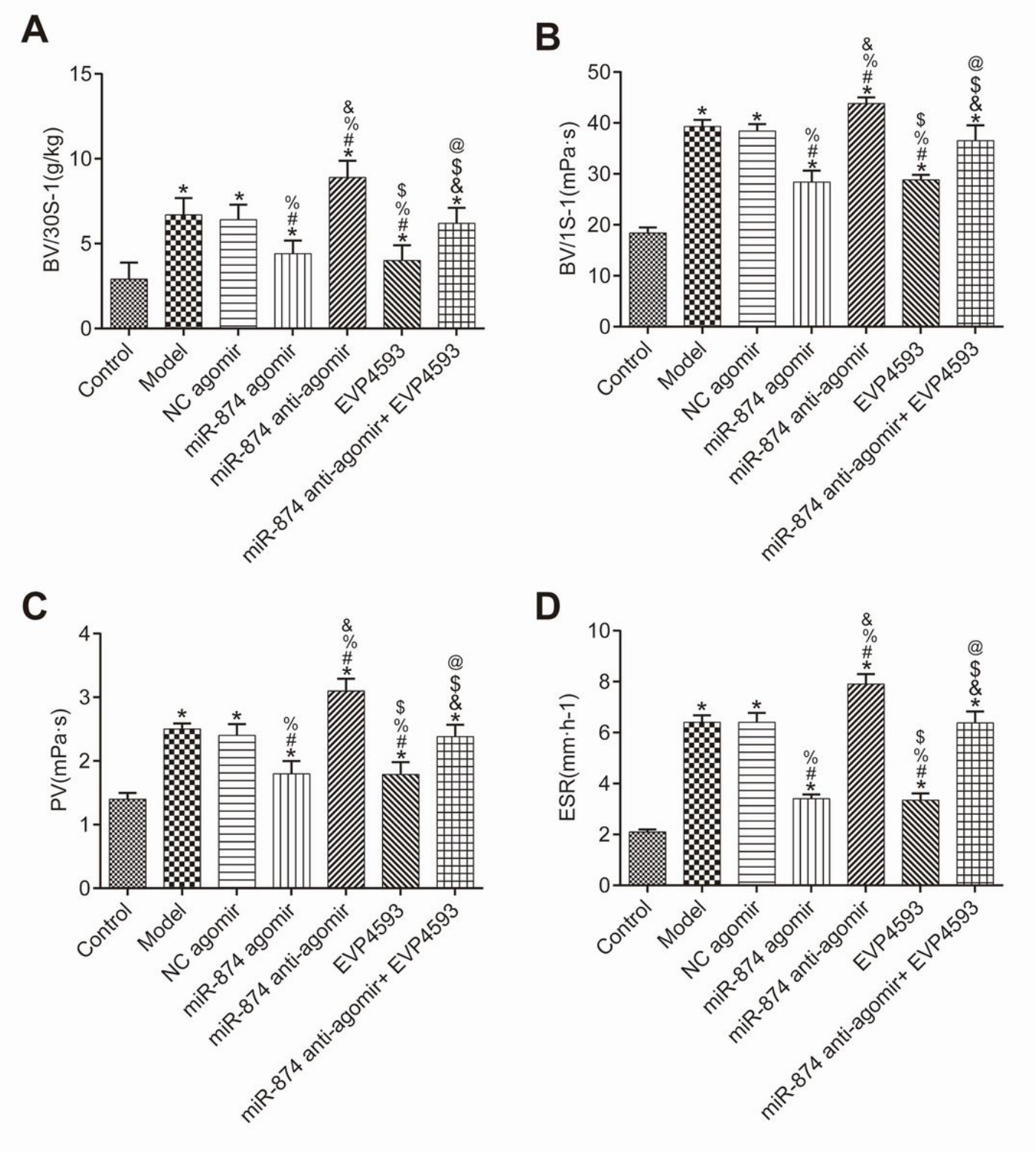

Figure 4

Retinal hemorheology of diabetes rats. A: BV/30s-1; B: BV/1s-1; C: PV; D: ESR. Compared with control group, *P < 0.05; compared with model group, #P < 0.05; compared with NC agomir group, %P < 0.05; compared with miR-874 agomir group, &P < 0.05; compared with miR-874 anti-agomir group, $P < 0.05; compared with EVP4593 group, @P < 0.05. NC negative control; BV blood viscosity; PV plasma viscosity; ESR erythrocyte sedimentation rate

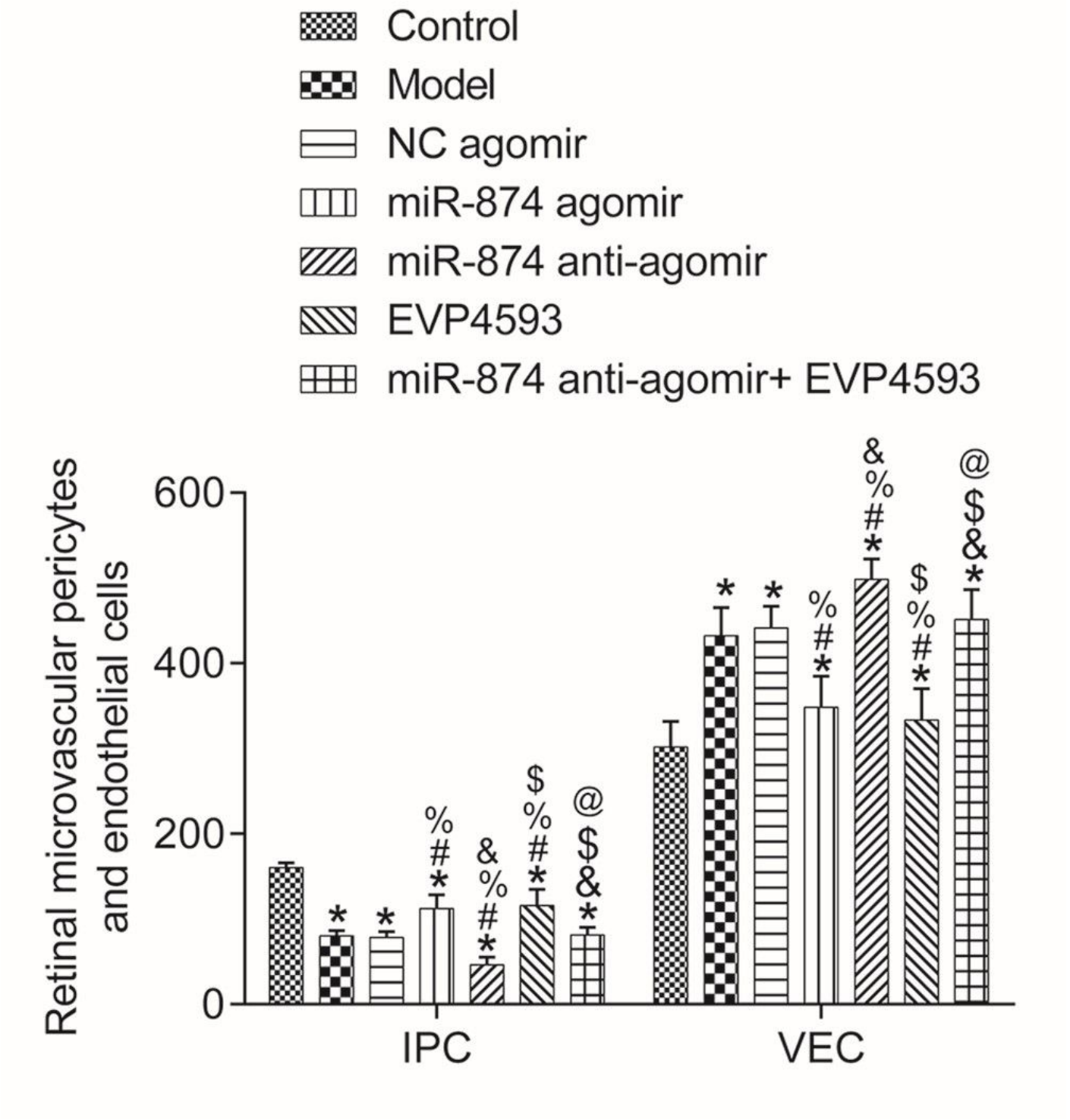

Figure 5

Number of retinal microvascular pericytes and endothelial cells. Compared with control group, number of retinal microvascular IPC was decreased, and number of VEC was increased in model group. Compared with control group, *P < 0.05; compared with model group, #P < 0.05; compared with NC agomir group, %P < 0.05; compared with miR-874 agomir group, &P < 0.05; compared with miR-874 anti-agomir group,

$P < 0.05; compared with EVP4593 group, @P < 0.05. NC negative control; IPC pericytes; VEC endothelial cells

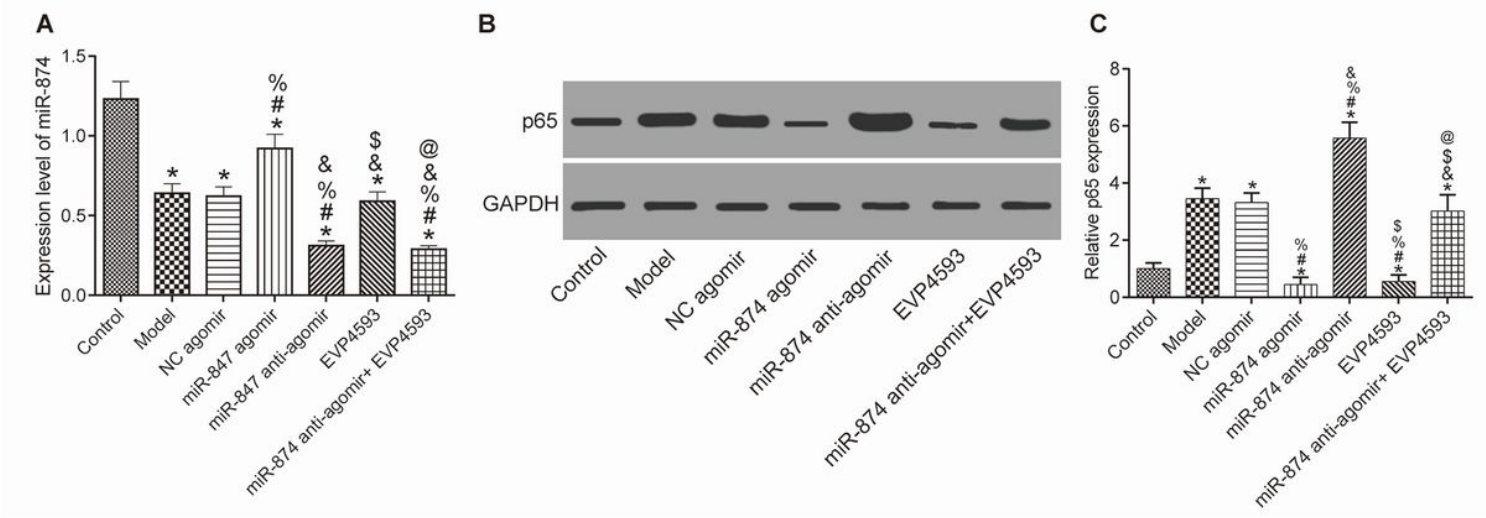

Figure 6

miR-874 and P65 expressions in the retina. A: miR-874 expression; B: Protein bands; C: Protein expression. Compared with control group, *P < 0.05; compared with model group, #P < 0.05; compared with NC agomir group, %P < 0.05; compared with miR-874 agomir group, &P < 0.05; compared with miR-874 anti-agomir group, $P < 0.05; compared with EVP4593 group, @P < 0.05. NC negative control

Supplementary Files

This is a list of supplementary files associated with this preprint. Click to download.

- NC3RsARRIVEGuidelinesChecklistfillable.pdf